Fluorescent cationic probes of mitochondria

Metrics and mechanism of interaction

James R. Bunting, Trung V. Phan, Eleanor Kamali, and Robert M. Dowben
The Baylor Research Foundation, Dallas, Texas 75226

ABSTRACT Mitochondria strongly accumulate amphiphilic cations. We report here a study of the association of respiring rat liver mitochondria with several fluorescent cationic dyes from differing structural classes. Using gravimetric and fluorometric analysis of dye partition, we find that dyes and mitochondria interact in three ways: (*a*) uptake with fluorescence quenching, (*b*) uptake without change in fluorescence intensity, and (*c*) lack of uptake. For dyes that quench upon uptake, the extent of quenching correlates with the degree of aggregation of the dye to dimers, as predicted by theory (Tomov, T.C. 1986. *J. Biochem. Biophys. Methods.* 13:29–38). Also predicted is the relationship observed between quenching and the mitochondria concentration when constant dye is titrated with mitochondria. Not predicted is the relationship observed between quenching and dye concentration when constant mitochondria are titrated with dye. Because a limit to dye uptake exists, in this case, the degree of quenching decreases as dye is added. A Langmuir isotherm analysis gives phenomenological parameters that predict quenching when it is observed as a function of dye concentration. By allowing for a decrease in membrane potential, caused by incorporation of cationic dye into the lipid bilayer, a modification of the Tomov theory predicts the dye titration data. We present a model of cationic dye–mitochondria interaction and discuss the use of these as probes of mitochondrial membrane potential.

INTRODUCTION

At the turn of the century, Michaelis discovered that the cationic dye Janus green B could be used for selective staining of mitochondria from other cellular organelles (1). Since then many dyes have been found to mimic the mitochondrial specificity of Janus green B (2). In 1946, Lewis et al. (3) observed that derivatives of the cationic mitochondrial specific dye brilliant cresyl blue preferentially stain tumor cells and retard their growth. More recently, applications of fluorescence microscopy have allowed the identification of novel fluorescent stains of intracellular organelles. The nontoxic fluorescent dye rhodamine 123 (Rh123) not only stains mitochondria specifically, but also, in a fashion similar to the cresyl blue of Lewis et al. (3) is taken up by, retained by, and inhibits growth of certain cancerous cells (4–7). The primary site of accumulation of these cationic dyes in the cell has been found to be in the mitochondria. The cell selectivity seen has been combined with the photosensitizing properties of aromatic dyes to yield photoactive anticancer therapeutic agents (8–10).

In light of the potential importance of mitochondrial specific antitumor agents, the interaction of aromatic cationic species with the mitochondria should be understood. We have undertaken a study of the interaction of aromatic amphiphilic fluorescent cations with respiring rat liver mitochondria. We wished to develop measures of the interaction of these cations with the mitochondria and understand differences which might be seen by these measurements. The primary measure that we have chosen to monitor is the fluorescence intensity decrease that occurs when many of these dyes interact with lipid bilayers possessing a transmembrane potential. The pioneering studies of Sims et al. (11) established cationic dyes as useful probes of membrane potential. They were the first to suggest that the reason for the quenching observed in fluorescence of cations interacting with membranes bearing potential was due to dimerization related quenching of the fluorescence. Loew et al. (12) proposed that the dimerization of DiSC2(5) was due to localized concentration of ions caused by potential forced diffusion of dyes into the interior space which the active membranes enclosed. Tomov (13) showed that the cationic dye, pyronin Y (PyY), behaves similarly to DiSC2(5) when added to isolated respiring mitochondria and, echoing the mechanism proposed by previous workers, developed a theoretical expression relating dye quenching to the dye dimerization constant, the mitochondrial volume present, the dye concentration added, and the membrane potential. Emaus et al. (14) performed a more comprehensive investigation of the relationship between the

Dr. Dowben is also Clinical Professor of Neurology at the University of Texas Southwestern Medical School, Dallas, TX.

0006-3495/89/11/979/15 $2.00

quenching of Rh123 added to mitochondria, and their metabolic and functional state. We expand the work here to other dyes. We have measured the change in fluorescence quenching observed as the cationic fluorophores are titrated with increasing concentrations of mitochondria, and when mitochondria are titrated with increasing concentrations of dye. We have tested the limits of the Tomov theoretical model in predicting the observed data, and out of necessity developed a correction to the Tomov theory, by including the effect on the membrane potential driving the sequestration caused by charge donated to the system by the mitochondrial localization of the dye. With this, a reasonable correlation between theory and observed titrations is obtained and we are provided with a set of measurables which describe the interaction of cations with mitochondria. The discussion outlines a model that attempts to integrate the observed data with mitochondrial function.

MATERIALS AND METHODS

Reagents

Dyes

Dyes from several general structural classes were used. Their chemical names, source and stated purity are given below.

Carbocyanine series. 1,1'-Diethyloxacarbocyanine iodide [DiOC2(3)], Molecular Probes Inc. (MP), Eugene, OR, >95%; 1,1'-diethyloxadicarbocyanine iodide [DiOC2(5)], MP, >95%; 1,1'-diethylthiacarbocyanine iodide [DiSC2(3)], MP, >95%; 1.1'-Diethylthiadicarbocyanine iodide [DiSC2(5)], MP, >95%.

Aminoxanthene series. Rhodamine 123 dihydrate (Rh123), Aldrich Chemical Co. (A), Milwaukee, WI, >99%; rhodamine 6G (Rh6G), A, >99%; rhodamine B (RhB), A, >99%; rhodanile blue (RAB), A, 85%.

Oxazine series. Oxazine 1 perchlorate (Ox1), Eastman Kodak Co. (K), Rochester, NY, >99%; oxazine 4 perchlorate (Ox4), K, >99%; Nile blue A perchlorate (NbA), K, >99%; cresyl violet perchlorate (CV), K, >99%.

Other ring systems. Safranin O (SafO), A, 95%; thionin (Th), A, 91%; pyronin Y (PyY), Matheson Coleman Bell, Cincinnati, OH, 58%.

A 1 mg/ml stock solution of each dye was prepared in absolute ethanol. The concentration was calculated from the absorbance of an ethanol-diluted aliquot using published extinction coefficients (15, 16). Immediately before use, working solutions of the dyes were prepared by dilution into working buffer, sucrose succinate buffer (SSB) with EGTA (described below), to a final concentration of 100 μM.

Other reagents

Buffer salts, sucrose, ethyleneglycol-bis-(aminoethyl ether) *N,N,N',N'* tetraacetic acid (EGTA), disodium succinate, rotenone, and carbonyl cyanide *m*-chlorophenylhydrazone (CCCP) were purchased from Sigma Chemical Co., St. Louis, MO. Tetraphenylphosphonium chloride (ϕ_4PCl) was from Aldrich Chemical Co.

Mitochondria isolation

Mitochondria from freshly excised liver of breeding retired male Sprague-Dawley rats were isolated at 4°C into 0.30 M sucrose by the method of Rickwood et al. (17). Delipidated bovine serum albumin (final concentration of 1.0 mg/ml) was added to the isolation medium during and subsequent to the second mitochondrial pelleting. Pellets were obtained by centrifugation at 12,000 *g*. Mitochondria were stored at 4°C at a concentration of ~50 mg/ml in a final isolation buffer (IB) containing 0.3 M sucrose, 1 mM EGTA, 0.1% BSA, 5 mM K_2PO_4, and 10 mM MOPS, adjusted to pH 7.4 with KOH. Mitochondrial concentration was estimated by Lowry's method of measuring protein (18), using lysozyme as standard. Mitochondrial integrity was determined by measuring the ATPase activity using the method of Pullman et al. (19). The regulatory control ratio measured oxygen consumption with a Clark's electrode (20). Upon addition of ADP and phosphate, mitochondrial preparations demonstrated a four- to sevenfold increase in oxygen consumption.

Experimental methods

Fluorometric measurements were performed on Farrand Optical Co. (Valhalla, NY) Mark I or Perkin Elmer Corp. (Norwalk, CT) model 502A spectrofluorometers using 10-nm band pass. All measurements were done at room temperature using SSB/EGTA containing 150 mM sucrose, 5 mM $MgCl_2$, 5 mM disodium succinate, 5 mM K_2PO_4, 2.5 μM rotenone, 1 mM EGTA, and 20 mM potassium-Hepes buffer (pH 7.4). Before addition of mitochondria, the wavelengths of maximal emission and excitation of the dye were adjusted to maximize the intensity of fluorescence relative to scatter (Table 1). The fluorescence signal was recorded on a strip chart.

Dyes were titrated with increasing amounts of mitochondria. (*a*) A stock solution of dye (1 mg/ml) was prepared in ethanol. Into 3.0 ml of SSB/EGTA, was added 30 μl of a 100 μM solution of working dye dilution, freshly prepared from stock into buffer. Total dye fluorescence was measured. (*b*) To the working dilution was added a sufficient volume of mitochondria stock suspension in IB (5–50 μl) to yield the final desired concentration of mitochondria. (*c*) After fluorescence changes plateaued, a reading of fluorescence observed (I_{obs}) was made. (*d*) The membrane potential was destroyed by addition of 30 μl of a 500 μM CCCP in SSB/EGTA, and I_{CCCP} was read. Subsequently, the light-scattering contribution to the signal was determined separately on a sample of mitochondria with no dye. The experimental metameter, ϵ, is the ratio of the intensity of fluorescence observed in the presence of mitochondria and dye (I_{obs}), divided by the total intensity of the sample observed after addition of CCCP, I_{CCCP}, corrected for scatter when necessary.

Constant amounts of mitochondria were titrated with dye by addition of sufficient volume of mitochondrial suspension in IB required (~25 μl) into 3.0 ml of SSB/EGTA to bring the final concentration of 0.1 mg/ml. Dye was brought to the final desired concentration by the addition of 30 μl of a 100X concentrate of dye in SSB, prepared fresh from stock, to 3.0 ml of the mitochondrial suspension. I_{obs} and I_{CCCP} were determined as above.

Inhibition of Rh123 binding by other dyes was accomplished by following the fluorescence change upon addition of sufficient stock mitochondrial suspension in IB to 3.0 ml SSB/EGTA to bring the final concentration to 0.1 mg/ml. The solution previously was made to contain a mixture of 1 μM Rh123 and the competing dye at an appropriate concentration. The sample was excited at 490 nm and the emission was monitored at 520 nm. I_{obs} and I_{CCCP} were determined as above.

Partition experiments were performed in duplicate. (*a*) Two samples of 0.1 mg/ml mitochondria were incubated with 1 μM dye until the fluorescence signal stabilized. I_{obs} was determined using the excitation and emission wavelengths listed in Table 1. (*b*) To one sample was then added 30 μl of 500 μM CCCP in SSB/EGTA and I_{CCCP} was determined. (*c*) Both samples were transferred into 1.5-ml microcentrifuge tubes

TABLE 1 Dye partition into mitochondria as a function of respiration

Compound	Fraction Bound − CCCP	Fraction Bound + CCCP	Reactive fraction, Fr	Quench factor, ϵ	Figure of merit, Fr(1-ϵ)	Wavelength (excitation, emission)
DiOC2(3)	0.75	0.12	0.84	0.72	0.24	475,500
DiOC2(5)	0.93	0.29	0.69	0.08	0.64	560,590
DiSC2(3)	0.93	0.22	0.77	0.92	0.06	550,590
DiSC2(5)	0.97	0.66	0.32	0.11	0.28	640,670
Rh123	0.57	0.00	1.00	0.39	0.61	470,525
Rh6G	0.80	0.10	0.89	0.59	0.37	530,550
RhB	0.13	0.11	0.16	1.00	0.00	540,575
RAB	0.11	0.05	0.50	1.00	0.00	550,580
Ox1	0.30	0.07	0.76	0.83	0.13	640,660
Ox4	0.02	0.02	0.00	1.00	0.00	610,625
NbA	0.43	0.42	0.01	1.00	0.00	625,670
CV	0.06	0.07	0.00	0.99	0.00	590,625
SafO	0.74	0.05	0.94	0.47	0.50	530,585
Th	0.20	0.20	0.00	0.89	0.00	600,620
PyY	0.84	0.19	0.77	0.28	0.56	550,570

See text for definitions.

and centrifuged at 14,000 *g* for 1.5 min. (*d*) The supernatant was removed from each tube and their remaining fluorescence recorded as I_{Sup+} and I_{Sup-} for supernatants with and without addition of CCCP, respectively. The fraction of dye uptake when the potential is present, F_+, was calculated as $1-(I_{Sup-}/I_{CCCP})$, the fraction of membrane potential unresponsive uptake, F_-, as $1-(I_{Sup+}/I_{CCCP})$, the fraction of total dye binding which is potential responsive, F_r, as $1-(F_-/F_+)$. A figure of merit for the dye as a fluorometric probe of membrane potential is given as the product of $F_r(1-\epsilon)$.

Calculation of fluorescence quenching titration curves using the Tomov expression

Tomov (13) modeled the quenching of fluorescence observed when a fluorescent dye is added to respiring mitochondria by taking the suggestion of Loew et al. (12) that the sequestration of the cationic dyes into the mitochondrial matrix space takes place under the electrophoretic force acting on the ion by its interaction with the transmitochondrial inner membrane potential. The higher local intramatrix concentration of dye forces dye aggregation and fluorescence quenching. Tomov derived a theoretical expression which related the transmitochondrial surface potential, E, to the concentration of suspended respiring mitochondria ([mito]), the concentration of fluorescent monocationic dye added to the suspension ($[D]$), the disaggregation constant of dye self-association (K_{Dm}), and an observable, the degree of quenching of dye fluorescence, ϵ, upon addition of the respiring mitochondria. His expression, rewritten using different symbols, is

$$E = 59 \log_{10} \{\delta(\epsilon(\delta(K_{Dm}/2[D])(1-\delta))^{-1/2} - 1)\} \quad (1)$$

The units of the variables are E, millivolts; K_{Dm} and $[D]$, molar. δ is a dimensionless ratio, equal to the mitochondrial matrix volume divided by the total suspension volume. It is estimated as the product of [mito] (milligrams per milliliter) and the volume of matrix per milligram of mitochondria, assumed for our calculations to be 0.001 ml/mg as measured by Harris and Van Dam (21).

Our purpose was to calculate ϵ as a function of variation in either δ or $[D]$, using the Tomov expression and an estimate of E, and K_{Dm}. Rearrangement of Eq. 1 gives a quadratic in ϵ:

$$\epsilon^2 + \epsilon b - b = 0, \quad (2)$$

where

$$b = (K_{Dm}\delta/2[D])((10^{(E/59)}/\delta) + 1)^2,$$

which is solved to yield ϵ.

Calculation of fluorescence quenching curves including the effect of charge screening on membrane potential

Heyer et al. (22) considered the effect of addition of amphiphilic cations, to one side of a lipid bilayer, on the monactin mediated, potassium ion conductivity across the bilayer, driven by a potential difference expressed across it. Fig. 1 presents a schematic diagram of the components in their system redefined to act as analogue to the mitochondrial inner membrane. Defined in the schematic are the applied or ionic diffusion transbilayer potential (V), the potential difference across the membrane proper (V_M), and surface potential on the mitochondrial matrix and cytosolic membrane faces, (Ψ_m and Ψ_c, respectively). These authors found that when they added amphiphilic cations to the cytosolic compartment, the presence of an applied membrane potential (negative on the matrix side) caused diffusion of the amphiphilic cation to the bilayer surface of the matrix, where it decreased the net negative fixed surface charge and thereby decreased the matrix face surface potential. The altered matrix face surface potential, when algebraically added to the cytosolic face surface potential and the electrode applied transmembrane potential, reduced the potential across the membrane proper and decreased the transport of monactin-K from cytosolic to matrix compartments.

Following their argument by analogy and with reference to the definitions of Fig. 1, the potential difference across the membrane

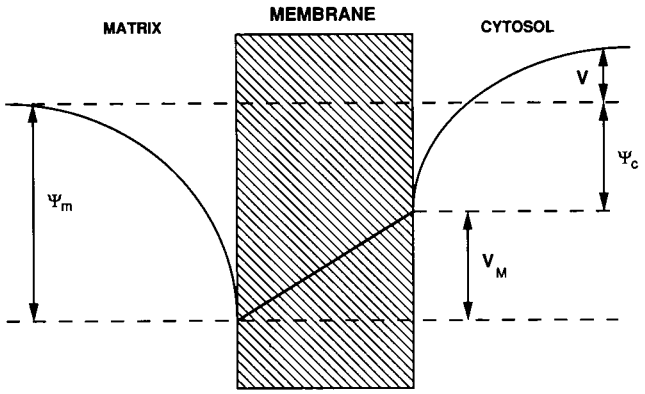

FIGURE 1 Electrostatics of mitochondrial inner membrane. V, applied or measured potential; Ψ_m, surface potential of matrix face; Ψ_c, surface potential of cytosolic face, V_M, transmembrane potential proper.

proper, V_M, is expressed as

$$V_M = V + (\Psi_m - \Psi_c). \quad (3)$$

In the case of our work, V is either an externally applied potential or a cationic diffusion potential. It is a fundamental assumption of the model presented here that the diffusion potential is not altered by dye binding: i.e., it is independent of the effects which occur at the membrane surfaces. With this assumption, an alteration in surface potentials, indicated by primes, will lead to an alteration in V_M:

$$\Delta V_M = (\Psi_{m'} - \Psi_m) - (\Psi_{c'} - \Psi_c). \quad (4)$$

As the cationic dye is introduced into the solution on the cytosolic side of the mitochondrial membrane, it is electrophoresed inward toward the matrix side. A much larger cationic concentration will reside near the matrix face surface; hence, the effect on the matrix surface potential caused by the addition of cationic charge to the fixed anionic surface charge will be much greater than on the cytosolic side, ie. $\Delta\Psi_m \gg \Delta\Psi_c$ and Eq. 5 may be simplified to:

$$\Delta V_M \simeq \Delta\Psi_m = (\Psi_{m'} - \Psi_m). \quad (5)$$

Heyer et al. (22) derived an expression for $\Delta\Psi_m$ as a function of the avidity of the cationic amphiphile's potential independent partition into the bilayer (β), the concentration of bulk monovalent cation in the matrix aqueous compartment ($[K]$), and the initial anionic surface charge density, σ_i. Their expression is rewritten with change in symbols as:

$$\Delta\Psi_m = 25.6[\ln\{(2S\beta\sigma_i[D] + [K] - (4S\beta\sigma_i[D][K] + [K]^2)^{1/2})/2(S\beta\sigma_i[D])^2[K]^{-1}\}]. \quad (6)$$

Our purpose was to utilize Eq. 6 to predict the effect of addition of cationic amphiphilic dyes on the mitochondrial matrix surface potential. Of first concern in utilizing Eq. 6 as a model of the mitochondria–dye interaction, an appropriate value for the initial matrix face anionic fixed charge, σ_i, must be assumed. We calculated it using the assumption that the full effective membrane potential, V_M, in mitochondria is expressed solely by a sufficiency of anionic fixed charge on the matrix side (i.e., $V_M = \Psi_m$). A second major assumption of the model is that variation at the matrix, not the cytosolic, surface potential is predominately responsible for changes in transmembrane potential. In support, we find little sensitivity of respiring mitochondrial uptake of Rh123 to increasing potassium or sodium ion concentration up to 200 mM in the incubating buffer (data not shown). Also, measurement of the mitochondrial surface potential gives only slightly negative values, no greater than -20 mV, which is little effected by the state of respiration (23, 24). Thus, a monovalent cationic concentration $[K]$ more typical of the matrix space of mitochondria (25) has been used throughout the calculations presented. Using a surface potential of -200 mV and $[K] = 0.1$ M, solution of the Gouy-Chapman expression, $4A^2\sigma_i = [K] \exp(-\Psi_{ie}/kT)$ (26), for σ_i gives a value of 6.4×10^{14} charges/cm^2. We used this value in calculations. The partition constant, β, was defined by Heyer et al. (22) as:

$$\sigma = \sigma_i - \beta[D],$$

where $[D]$ is the total cationic dye concentration "at the membrane surface," and σ is the new anionic surface charge after partition into the surface. The units of β are charges cm^{-2} M^{-1}. Heyer et al. measured β for the longchain quaternary n-methylaminoalkyl cations (QA) and found them to range from 4.2×10^{15} for nonyl-QA to 2.4×10^{17} for dodecyl-QA partitioning from aqueous phase into phosphatidylglycerol/cholesterol (50%:50%) bilayers. There is evidence in the literature to support the contention that the values of β for amphiphilic aromatic ions into lipid bilayers is not much different than those for the quaternary ammonium lipids studied by Heyer et al. If one assumes that $\beta = (\text{esu/cm}^2)/K_d$, then a β of 7×10^{18} esu cm^{-2} M^{-1} is calculated from a K_d of 2×10^{-4} M and 1 esu/70 Å^2 as reported by McLaughlin and Harary (27) for the partition of toluidinylnaphthalene sulfonate into phosphatidylcholine bilayers. Likewise a β of 3×10^{18} is calculated from the data of Gibrat et al. (28) for partition of carbonyl p-trifluromethoxyphenylhydrazone cation and 6.6×10^{15} for tetraphenyl phosphonium ion into soy lecithin bilayers. S is a constant of proportionality which at 300°K has the value 7.3×10^{-28} M cm^4 per charge. As the units of S are unusual, an explanation of its calculation is in order. Heyer et al. (22) define S in a statement of the Poisson-Boltzmann equation for large surface potentials in the presence of only uni-univalent salts as $S\sigma_i = [K] \exp(-\Psi_i e/kT)$. The Gouy-Chapmann expression (26) is written as $4A^2\sigma_i = [K] \exp(-\Psi_i e/kT)$, where Ψ_i is the surface potential, e the electron charge, k the Boltzmann's constant, and T the Kelvin temperature. Thus $S = c4A^2$, where c is 10^{32} cm^4 Å^{-4} needed to convert the length units of Ångstroms in A to centimeters in S. Using a value of 135.1 for A at 300°K (tabulated in the review of McLaughlin and Harary [26]), S is calculated to be as stated above.

The effect on the fluorescence quenching of adding increasing cationic dye to constant mitochondria was modeled by assuming that the addition of dye decreases the effective surface potential on the matrix side by an amount calculated using Eq. 6. This surface potential change causes a decrease in the transmembrane potential proper, which changes the degree of concentration and aggregation of the dye in the matrix, as reflected by a decrease in E of Eq. 2, i.e.,

$$E = E_o + 25.6[\ln\{(2S\beta\sigma_i[D] + [K] - (4S\beta\sigma_i[D][K] + [K]^2)^{1/2})/2(S\beta\sigma_i[D])^2[K]^{-1}\}], \quad (8)$$

which, given σ_i, β, and E_o, was solved for E as $[D]$ was increased. The value of E so obtained was inserted into Eq. 2 and the quenching parameter, ϵ, was computed.

Determination of Langmuir binding parameters and their use in prediction of fluorescence quenching titration curves

Apparent Langmuir binding parameters describing the uptake of dye by mitochondria were extracted from fluorescence data using the method of Bashford and Smith (29). The fraction of total dye added which is bound to the mitochondria, C, is related to the fluorescence quenching parameter, ϵ, by:

$$C = (1 - \epsilon)/(1 - \epsilon_b), \quad (9)$$

where ϵ_b is the maximal quenching of dye observed at infinite mitochondrial concentration. ϵ_b is estimated from the titration data after quenching as the mitochondrial concentration is increased, using the relationship:

$$1/(1 - \epsilon) = 1/(1 - \epsilon_b) + K_d/((1 - \epsilon_b)n[\text{mito}]), \quad (10)$$

where K_d (M) is the dye to lipid Langmuir absorption constant, n is the maximum number of moles of mitochondria dye binding sites per milligram (mmol/mg), and [mito] is the milligrams per milliliter concentration of mitochondria added at constant dye concentration. A plot of $(1 - \epsilon)^{-1}$ vs. $[\text{mito}]^{-1}$ gives $(1 - \epsilon_b)^{-1}$ at the intercept. Once ϵ_b has been calculated, K_d and n can be determined from the relationship:

$$1/\sigma = 1/n + K_d/(n)[D]_f, \quad (11)$$

where σ (mmol/mg) is the number of moles of dye molecules bound per milligram of mitochondria added and $[D]_f$ is the free dye concentration at equilibrium. σ is calculated as $[D]_b/[\text{mito}]$, where $[D]_b$ (moles/liter) is equal to $C[D]$, where C is the bound over total ratio calculated from experimental data using Eq. 9. $[D]_f$ is calculated as $(1 - C)[D]$, where $[D]$ is the total dye concentration added. A plot of σ^{-1} vs. $[D]_f^{-1}$ gives n^{-1} as the intercept and K_d/n as slope, from which K_d is calculated.

Increasing the dye/protein ratio above a certain level (see Fig. 7) results in decrease of the dye binding; therefore, we performed the determination of Langmuir parameters by holding the dye concentration constant at 1 μM and varying the amount of mitochondria added to SSB/EGTA starting at a protein/dye ratio below that seen to effect the maximal quenching and proceeding to higher amounts of protein added. The Langmuir parameters thus obtained represent the situation at low dye loads.

Having obtained estimates of K_d and n, we used a rearrangement of Eq. 9 to calculate a prediction of ϵ as [mito] or $[D]$ is increased:

$$\epsilon = C(\epsilon_b - 1) + 1, \quad (12)$$

where C was obtained from solution of a back transform of Eq. 11:

$$C^2 - C[1 + K_d[\text{D}]^{-1} + n[\text{mito}][D]^{-1}] + n[\text{mito}][\text{D}]^{-1} = 0$$

RESULTS

Dye titration with respiring mitochondria

Curve A of Fig. 2 shows the effect of increasing the concentration of succinate activated respiring rat liver mitochondria on the fluorescence quenching of 1 μM Rh123. An ϵ of unity indicates no quenching occurred; a fractional value indicates quenching. The downward concave shape of the curve can be broken into three regions. At low mitochondria concentration, the ratio of dye to mitochondria is high, and all dye potential-dependent bound dye is assumed to be quenched. On this leg of the curve, the membrane potential-independent absorption of the dye into the membrane will also be highest. As mitochondrial concentration increases, a maximum level of quenching is reached, reflecting some optimal partition of dye into mitochondria for the expression of quenched fluorescence. At mitochondrial concentrations above this, an increasing sufficiency of mitochondrial volume dilutes out the process causing quenching. Curve B in Fig. 2 resulted when Rh123 concentration was reduced to 10 nM and then titrated with mitochondria. Here, the general shape is maintained, but the maximum quenching decreases and the mitochondria concentration at maximum quenching shifts lower.

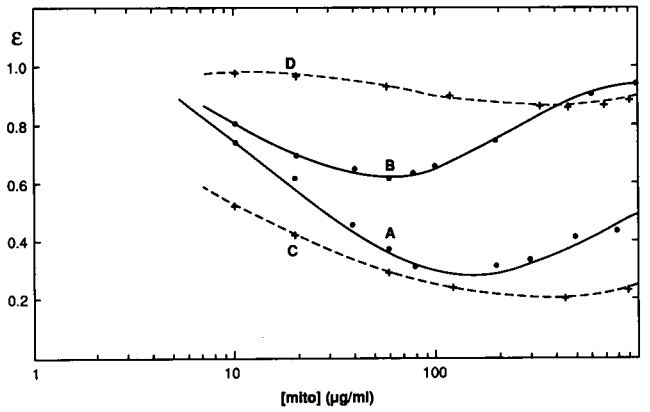

FIGURE 2 Comparison of observed and theoretical changes in fluorescence quenching of dye at constant concentration in SSB/EGTA upon addition of mitochondria. (A and B) Observed upon addition of mitochondria to 1 μM Rh123 and 10 nM, respectively. (C and D) Calculated using Eq. 7 with $K_{Dm} = 7 \times 10^{-5}$ M and $E = -200$ mV for dye concentration of 1 μM and 10 nM, respectively.

The Tomov equation (Eq. 2) was used to simulate quenching as a function of mitochondrial concentration. Fig. 3 A shows a family of curves of quenching factor as a function of the log of mitochondrial concentration obtained by solving Eq. 2 with the membrane potential and cationic dye concentration added fixed at -200 mV and 1×10^{-6} M, respectively, and the dye dimerization disassociation constant, K_{Dm}, varied. As with the experimentally determined curve of Fig. 2, there is a downward concavity whose maximum position on the [mito] axis does not move as K_{Dm} is decreased but rather its value

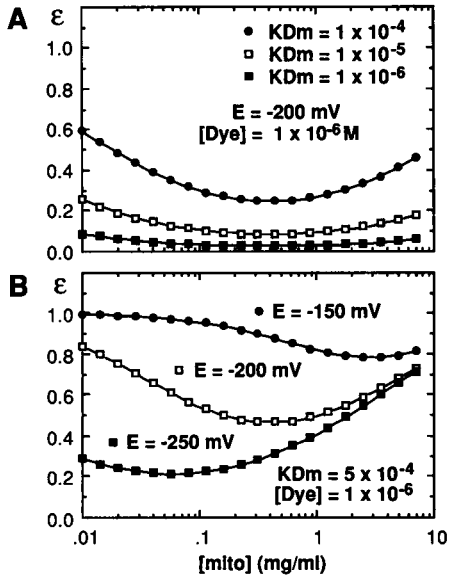

FIGURE 3 Tomov equation. Theoretical fluorescent quenching vs. mitochondria concentration. K_{Dm}, dye disaggregation constant; E, transmembrane potential; [Dye], concentration of fluorescent cation added; [mito], mitochondrial concentration. (*A*) Variation in K_{Dm}, E, and [Dye] constant. (*B*) Variation in E, K_{Dm}, and [Dye] constant.

decreases (more quenched) and flattens the curve concavity. Fixing K_{Dm} at 5×10^{-4} M (a value typical of the cationic dyes investigated) and fixing $[D]$ at 1×10^{-6} M, a family of curves seen in Fig. 3 *B* is obtained as the membrane potential assumed is intensified from -150 to -250 mV. Here the [mito] at maximum quenching (minimum ϵ) is seen to be a sensitive function of potential, moving almost an order of magnitude for each 50-mV change. Reduction of the [Dye] in the calculations simply flattens and elevates the effects seen in Fig. 3.

Assuming a value for the membrane potential of -200 mV, and [Dye] of 1 μM, a search was made for a value of K_{Dm} which, when applied to Eq. 2, would match the maximum degree of quenching (minimum ϵ) calculated to that observed for titration of 1 μM Rh123 (Fig. 2, curve *A*). Curve *C* of Fig. 2 was calculated with $K_{Dm} = 7.0 \times 10^{-5}$ M. It yields a slightly smaller quench factor minimum value located at higher [mito] than that observed. With this value of K_{Dm}, $E = -200$ mV and reducing the [Dye] to 10 nM, Eq. 2 calculates curve *D* in Fig. 2. Here we see major disagreement between theory and observed. The theoretical minimum of ϵ for the 10 nM case is directly over that of the 1 μM case, although the depth has been much reduced. The [mito] observed for 10 nM dye titrated is shifted to lower [mito] than either the observed 1 μM case (curve *A*) or the calculated 10 nM case (curve *D*). The differences between theory and observation must be due to other factors which either (*a*) enhance the quenching at lower dye loading or (*b*) inhibit the dye binding at higher dye to mitochondria ratios to a degree greater than that predicted by the assumptions of the Tomov theoretical treatment. The greater calculated sensitivity of [mito] at maximum quenching to changes in the membrane potential suggest that the binding of the dye itself affects the membrane potential.

To test further the predictability of the Tomov expression, a group of dyes that possess differences in dimerization constant were titrated with increasing amounts of mitochondria (Fig. 4). The disaggregation constant of PyY has been measured as 7.0×10^{-4} M (13), and for DiSC2(5) as 1.5×10^{-5} M (30). Based on increased aromatic and aliphatic surfaces in the structure of Rh6G as compared with PyY, the disaggregation constant for R6G is expected to be intermediate between that of PyY and DiSC2(5), probably somewhere about that of thionin reported to have a disaggregation constant of 2.8×10^{-4} M (31). Because of the close similarity between the structures of DiOC2(5) and DiSC2(5), one would expect them to have similar dimerization tendencies. The curves of Fig. 4 confirm that the degree of maximum quenching increases inversely proportional to the disaggregation constant, as predicted: DiSC2(5) $\simeq$ DiOC2(5) > R6G > PyY; $1.5 \times 10^{-5} < 1 \times 10^{-4}$ (estimated) $< 7.0 \times 10^{-4}$ M. PyY and Rh6G both demonstrate a maximum quenching at ~170 μg/ml mitochondria added to 1 μM dye. For DiOC2(5) the maximum quenching is shifted to ~100 μg/ml, and the concavity width is increased. A further accentuation of maximal quenching is seen for DiSC2(5) where the quenching is high and flat at low mitochondrial concentrations. This behavior is not predicted by the Tomov expression. We wondered whether the deviation in observed vs. theoretical titration curves might depend on the relative lipid solubility of the dyes. If lipophilicity

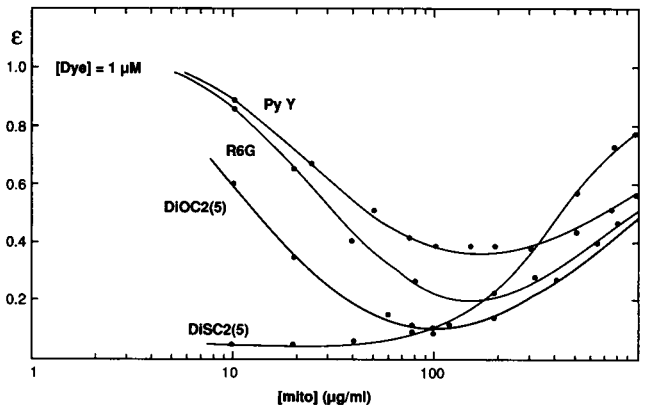

FIGURE 4 Change in fluorescence quenching of dyes upon addition of increasing amount of dye to 0.1 mg/ml mitochondria in SSB/EGTA. Dye abbreviations given in Materials and Methods.

were high, quenching might be enhanced at lower mitochondrial concentrations because the net dye concentration at the lipid–aqueous interface where dimerization occurs would be higher than expected.

Partition of dyes into mitochondria as a function of membrane potential

By gravimetric partition experiment, the extent of cationic dye uptake that is both dependent and independent of the presence of membrane potential was measured. Dye and mitochondrial concentration were held constant at 1 μM and 0.1 mg/ml, respectively, and the amount of dye absorbed in the absence (membrane potential present) and presence (membrane potential collapsed) of 2.5 μM CCCP was determined by analyzing the loss of dye fluorescence in the supernatant of the suspension after pelleting the mitochondria by centrifugation (Table 1). As a control, the zwitterionic dye rhodamine B (RhB) was included. The data indicate that both DiSC2(5) and DiOC2(5) partition appreciably into mitochondria in the absence of a membrane potential to a degree of 0.66 and 0.29, respectively, whereas Rh123 and PyY only partition to 0.00 and 0.19 in the absence of membrane potential. A reactive fraction was calculated which represents the fractional uptake of the total dye that is responsive to the presence of membrane potential. Rh123, DiOC2(3), DiSC2(3), Ox1, and Rh6G all have a reactive fraction >0.75, indicating that most of the partition is potential-dependent. Good potential-dependent partition, however, does not necessarily equate to high efficacy as a membrane potential fluoroprobe because the degree of dye self-association within the potential reactive fraction is a factor, as well as dye dark and phototoxicity effects which may be present. We calculate (Table 1) a figure of merit to reflect the relative utility of a cationic fluorophore as membrane potential probe as the product of the potential reactive fraction and the dynamic range of quenching observed, $(1 - \epsilon)$. The best probe should be chosen to have a figure of merit as close to 1.0 as possible. Reassuringly, those dyes that are routinely successful as membrane potential fluoroprobes, PyY, Rh6G, Rh123, and DiOC2(5), all have a figure of merit >0.5. In contrast, although greatly quenched upon partition, DiSC2(5) contributes largely to the quenching associated with potential-independent partition and thus has a low figure of merit, 0.28. Oxazine 1, although showing good partition with limited potential independent partition, does not quench upon uptake. Oxazine 4 neither binds nor quenches. Nile blue A, also an oxazine dye, partitions into mitochondria in a fashion that is potential independent and exhibits no fluorescence quenching. Its lipophilicity reflects its use as a general stain for fat cells (2). The peculiarity of the oxazines is not understood. They should have dimerization constants comparable to the other dyes tested. Possibly they are binding to some specific site within the concentrated intramitochondrial space and are kept from interaction, or are simply destroying the membrane potential by poisoning the potential generating machinery.

To investigate dye toxicity on mitochondrial respiration, the rate of oxygen consumption of mitochondria treated with dye was followed using a Clark's electrode. Mitochondria were added to analysis buffer (10 mM KP_i, 0.225 M sucrose, 5 mM $MgCl_2$, 20 mM KCl, 20 mM triethanolamine, pH 7.4) to a final concentration of 1 mg/ml. The basal rate of oxygen consumption prior to other additions was measured. Then cationic dye was added to a final concentration of 10 μM (yielding the same dye/mitochondrial ratio as 1 μM/0.1 mg/ml) and the oxygen utilization rate followed for a period of time.

TABLE 2 Effect of cationic dyes on mitochondrial respiration

Dye	O_2 consumption rates*			No.	Respiratory control ratio	Significance* of RCR
	Basal	+Succinate	+ADP			
	ng atoms O_2/min/mg/ml				*rate + Succ/rate + ATP*	
None	0.1	0.58 ± 0.12	2.7 ± 1.1	8	4.6 ± 2.1	—
Rh123	0.1	0.68 ± 0.20	1.4 ± 0.6	6	2.0 ± 1.1	$P < 0.05$
Th	1.2	2.7 ± 0.50	4.3 ± 1.6	2	1.6 ± 0.7	$P < 0.01$
RhB	0.1	1.0 ± 0.40	3.9 ± 1.1	2	3.9 ± 1.9	NS
RAB	0.1	0.90 ± 0.20	2.8 ± 0.5	2	3.2 ± 0.9	$P < 0.20$
Ox4	0.1	1.1	1.4	1	1.3	$P^{\ddagger} < 0.10$
NBA	0.1	1.4 ± 1.5	2.0 ± 1.5	2	1.5 ± 1.2	$P < 0.05$
CV	0.1	1.8	2.8	1	1.6	$P^{\ddagger} < 0.10$
DiOC2(3)	0.1	0.8	2.8	1	3.64	NS

Errors calculated following the method of Beers (32).

*Two-tailed t test (33) testing the hypothesis that the mean of the tested and control populations are equal.

‡Estimated assuming the standard error of estimate is the average of the standard errors calculated for the other RCRs.

Disodium succinate was then added to a final concentration of 10 mM and the rate of "state IV" oxygen consumption rate was measured, after which ADP was added to a final concentration of 400 μM and the "state III" oxygen consumption rate was measured. Table 2 shows the results of these experiments. The general effect of dye addition on the rate of succinate limited respiration (state IV) is to stimulate it. The effect of dye addition on the rate of [ADP] limited respiration (state III) was varied. Rh123 addition reduced the rate of oxygen consumption to half the control value; addition of thionin, however, appeared to double the rate. The respiratory control ratios calculated show that they are either reduced by the presence of the dye or leave it relatively untouched. Thionin is unique in the fact that addition of it alone stimulated the basal, presuccinated addition, and the subsequent addition of reagents perpetuates this stimulation. Dyes that appeared to poison mitochondria to their uptake, CV, Ox4, removed respiratory control but did not interfere with oxygen consumption.

Titration of mitochondria with dye

When mitochondrial concentration is held at 0.1 mg/ml and Rh123 is added in increasing amounts, ϵ varies (Fig. 5). The points plotted represent observations, while the dotted line is that predicted by the Loew-Tomov theory, Eq. 2 solved using $E = -200$ mV, $K_{Dm} = 7.0 \times 10^{-5}$ M, and a mitochondrial concentration of 0.1 mg/ml. Clearly, the observed relationship is not supported by theory. In the Tomov theory, no limits exist for the amount of dye that can be sequestered. An increase in the bulk dye concentration continues to increase the intramitochondrial dye concentration in a proportional manner, causing further dimerization and quenching.

As dye is added, the increase in ϵ toward unity may be modeled phenomenologically assuming that a Langmuir isotherm absorption of dye to mitochondria is occurring. This relationship relates the degree of dye binding to the apparent equilibrium disassociation constant, K_d (molar), and an apparent limiting number of binding sites, n (moles per milligram). The low mitochondrial concentration leg of the quenching data was obtained upon titration of dye with mitochondria (Fig. 2) and was analyzed by the method of Bashford and Smith (29) (See Experimental Methods subsection). Fig. 6 *A* shows the double reciprocal plot of $(1 - \epsilon)^{-1}$ vs. $[\text{mito}]^{-1}$ for binding of 1μM Rh123 to increasing mitochondria. This plot in turn was used to estimate a limiting quenching constant, ϵ_b of 0.28. Using this value for calculation of σ and free dye concentration, Fig. 6 *B* was constructed to estimate a dissociation constant, K_d, of 4.8×10^{-7} M and a capacity, n, of 48 nmol/mg. With these estimated parameters, Eq. 12 was solved for increasing concentration of dye added and yielded the solid curve of Fig. 5. Good agreement between theory and observed data is obtained using these estimated parameters. Similar analyses were performed on the binding data for 10 nM Rh123, RH6G at 1 μM and 10 nM, and DiOC2(5) at 1 μM (Table 3). The dissociation constant is decreased in proportion to the dye concentration by a factor of 10^{-2} (from 1 μM to 10 nM Rh123). This is expected from the Gouy-Chapman relationship, as the effective surface concentration of dye delivered $[D]$ is proportional to $[D]10^{(-E/59)}$. In compari-

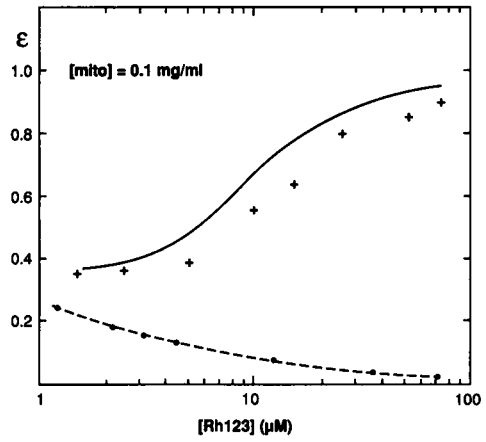

FIGURE 5 Observed and theoretical changes of fluorescence quenching upon addition of increasing amounts of Rh123 to 0.1 mg/ml mitochondria in SSB/EGTA. (+) Observed quenching. (*Solid line*) Theoretical assuming Langmuir isotherm using Eq. 4 with $K_d = 2.1 \times 10^6$ and $n = 48$ nmol/mg. (*Dashed line*) Theoretical using Eq. 2 with $K_{Dm} = 7 \times 10^{-5}$ M and $E = -200$ mV.

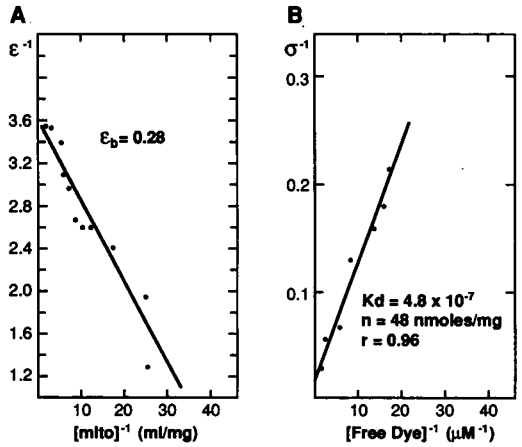

FIGURE 6 Double reciprocal plots for estimate of Langmuir isotherm parameters K_d and n for binding to Rh123 to mitochondria. (*A*) Determination of limiting quenching factor, ϵ_b. (*B*) Determination of K_d and n. See Materials and Methods for details.

TABLE 3 **Summary of Langmuir isotherm binding constants**

Compound	Concentration (μM)	Dissociation Constant, K_d	Binding Capacity, n
		M	*nmoles/mg*
Rh123	1.0	$4.8 \pm 2.0 \times 10^{-7}$	48 ± 6
Rh123	0.01	$5.0 \pm 3.2 \times 10^{-9}$	1.25 ± 2.2
Rh6G	1.0	$1.8 \pm 1.7 \times 10^{-7}$	25 ± 11
Rh6G	0.01	$3.4 \pm 2.4 \times 10^{-9}$	0.5 ± 1.6
DiOC2(5)	1.0	$1.4 \pm 2.2 \times 10^{-7}$	55 ± 5

Errors represent estimates from the statistics of linear regression analysis.

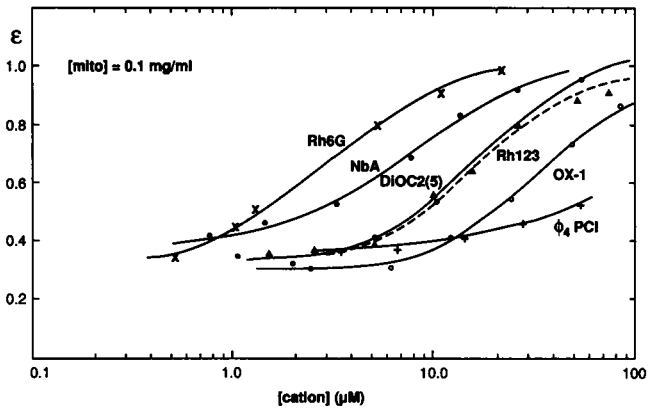

FIGURE 7 Effect on fluorescence quenching of 1 μM Rh123 added to 0.1 mg/ml mitochondria in SSB/EGTA by addition of increasing amounts of other aromatic cations. Dashed line is for self-titration with Rh123 for comparison. Abbreviations given in Materials and Methods.

son, Rh6G titrated at 10 nM has a slightly higher dissociation constant than 10^{-2} times the K_d at 1 μM and has a lower capacity for binding compared to 10 nM Rh123. This suggests that some other modulator of the interaction with mitochondria is in effect with Rh6G. The Langmuir parameters are phenomenological, however, and do not give an indication of the nature of the saturation process. What is apparent is that the Waggoner–Loew–Tomov model is incomplete since prediction of the binding of dye to mitochondria depends on a limiting capacity for dye uptake.

Inhibition of Rh123 binding by other organic cation species

In order to probe the saturation effect more fully, we measured the fluorescence quenching of 1 μM Rh123 in the presence of 0.1 mg/ml of mitochondria, as a function of co-addition of increasing concentrations of other aromatic cationic dyes (Fig. 7). The dotted curve is the self-inhibition of Rh123 for a comparison point. Inhibition of Rh123 binding generally correlates with the partition observed for the dyes in the absence of membrane potential (Table 1). The relationship is not perfect; e.g., a greater inhibition of binding is expected for DiOC2(5) than is observed. However, if the quenching of Rh123 fluorescence is assumed to be in proportion to the size of the membrane potential, then the data suggest that binding of another dye is itself responsible for a decrease in effective membrane potential.

A theoretical model, a modification of the Tomov approach, was developed in which the membrane potential becomes a function of the dye concentration added. Support for this approach exists in work relating to the interaction of cationic anesthetics with anionic and dipolar lipid bilayers. Adsorption of a mobile lipophilic cationic species to the aqueous–lipid interface area of fixed anionic surface charged lipid bilayers reduces the effective fixed anionic surface charge causing a decreased membrane potential (26). Heyer et al. (22) developed an expression (Eq. 6) relating the change in surface potential as a function of the partition coefficient of a lipophilic cationic species entering the lipid, the bulk cationic dye concentration, the surface density of anionic charge on the bilayer, and the membrane potential prior to addition of cationic absorbing species. Solution of Eq. 8 yields a membrane potential, E, representing the new membrane potential after the surface absorption of the mobile cationic species, in terms of its original potential before dye addition, E_o (see Experimental Methods subsection for details). The altered membrane potential, E, so obtained is substituted into the Tomov expression (Eq. 2) which is then solved for ϵ. The relationship between quenching parameter and the concentration of dye added to a given mitochondrial concentration depends on three estimable and potentially measurable physical constants: the initial membrane potential, E_o, the partition coefficient of cationic dye lipophilicity, β, and the disaggregation constant for dye dimerization, K_{Dm}. Fig. 8 *A* shows a family of curves of ϵ vs. log[Dye] calculated in this fashion as E_o and β are held constant at -200 mV and $1 \times 10^{+18}$ charges per cm^2/M, respectively, and the dimerization disaggregation constant is varied from 1×10^{-4} to 1×10^{-6} M. Theory predicts the observed increase in quenching factor toward unity as dye concentration is increased. As the disaggregation constant is varied, theory predicts that as the tendency of dimerization increases, ϵ at low dye concentration decreases. Also observed is that variation of K_{Dm} did not affect the dye concentration at which the range of ϵ is half-maximal. As the cationic dye lipophilicity is varied, i.e., as β is increased from 1×10^{16} to 1×10^{19} charges per cm^2/M, and where $E_o = -200$ mV and $K_{Dm} = 1 \times 10^{-5}$ M are held

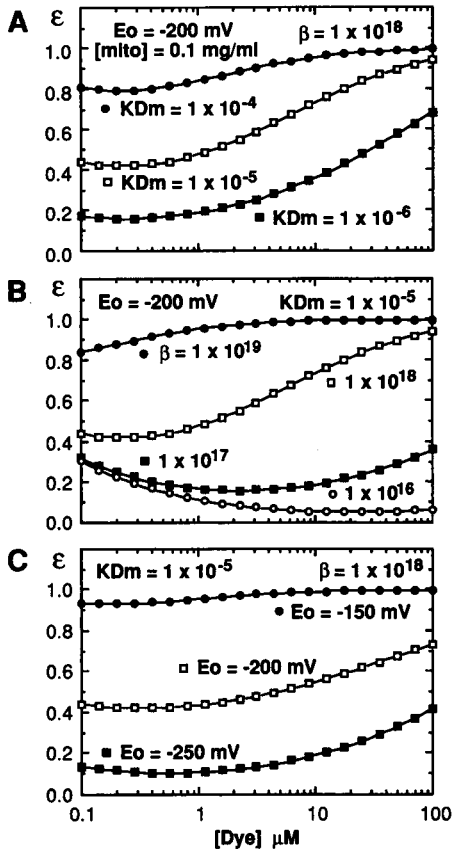

FIGURE 8 Heyer–Tomov equation, theoretical fluorescent quenching vs. dye concentration. β, cation/lipid partition constant; E_o, original transmembrane potential; other symbols as defined in Fig. 3. (*A*) Variation in K_{Dm}; other parameters constant as indicated. (*B*) Variation in β, others constant. (*C*) Variation in E_o, others constant.

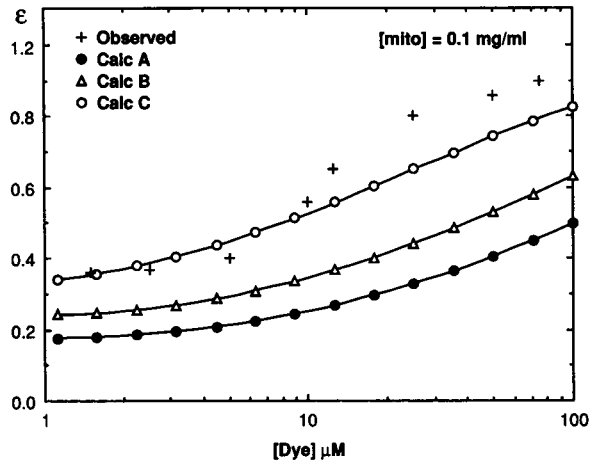

FIGURE 9 Tomov-Heyer equation, theoretical solutions compared to observed data. (+) Observed for Rh123 titration of 0.1 mg/ml respiring mitochondria. (Calculated *A*) Calculated: $E_o = -210$ mV, $K_{Dm} = 1 \times 10^{-5}$ M, $\beta = 2.5 \times 10^{17}$ ch/cm^2/M. (Calculated *B*) Calculated: $E_o = -200$, $K_{Dm} = 1 \times 10^{-5}$ M, $\beta = 2.5 \times 10^{17}$. (Calculated *C*) $E_o = -200$, $K_{Dm} = 1 \times 10^{-5}$, $\beta = 5 \times 10^{17}$.

constant, the theory predicts the changes in ϵ vs. log[Dye] seen in Fig. 8 *B*. The case where cation is least lipophilic, $\beta = 1 \times 10^{16}$, results in an ϵ vs. log[D] plot as predicted by the Tomov theory (See Fig. 6, *dashed curve*). As the cation lipophilicity is increased, theory predicts that ϵ at higher [*D*] begins to increase leading to a sigmoidal shaped relationship between ϵ and log[*D*]. The shape and inflection points of ϵ vs. log[*D*] are a sensitive function of β. Finally, theory predicts that as E_o is increased from -150 to -250 mV, keeping $\beta = 1 \times 10^{18}$ and $K_{Dm} = 1 \times 10^{-5}$, the depth, but not the shape factor of the ϵ vs. log[Dye] curve predicted is increased, as seen in Fig. 8 *C*.

Again, a search for estimated parameters which yielded reasonable fit to experiment was performed. Fig. 9 demonstrates the results of this graphical search. Since the degree of quenching was seen to be relatively unaffected by change in value, a value of 1×10^{-5} M was chosen as an estimate for K_{Dm} representing an average of the literature reported values for the cationic dyes. Using this disaggregation constant, and a value of 2.4×10^{17} for β, a value measured for partition of *N*-(tetramethyl) dodecylamine into simple lipid bilayers by Heyer et al. (22), the theoretical curve for the case where $E_o = -210$ and -200 mV is seen as Fig. 9, *A* and *B*, respectively. Although increasing E_o to a higher value than expected did lift the ϵ at low [Dye] closer to that observed, the inflection point of the theoretical curve and the observed do not match. Keeping K_{Dm} at 1×10^{-5} M, E_o at a more typical -200 mV but increasing β to 5×10^{17} results in Fig. 9 *C*. Here a fair match is obtained between theory and observation. This is not a unique solution, but at least one which uses reasonable first guesses of the physical parameters involved.

DISCUSSION

A diagram depicting a possible model for the interaction of cationic aromatic moieties with respiring mitochondria which follows from the results is seen in Fig. 10. The dyes are assumed to interact primarily with the lipid–aqueous interfacial regions of the inner membrane. In *A*, in the absence of a membrane potential (in the presence of CCCP), the charge density is equal for fixed anions on both the external and internal mitochondrial faces so that no net transmembrane potential is generated. Under these conditions, dye can partition into the outer surface of the inner mitochondrial membrane with an apparent association constant, *K*, to give a concentration of dye in

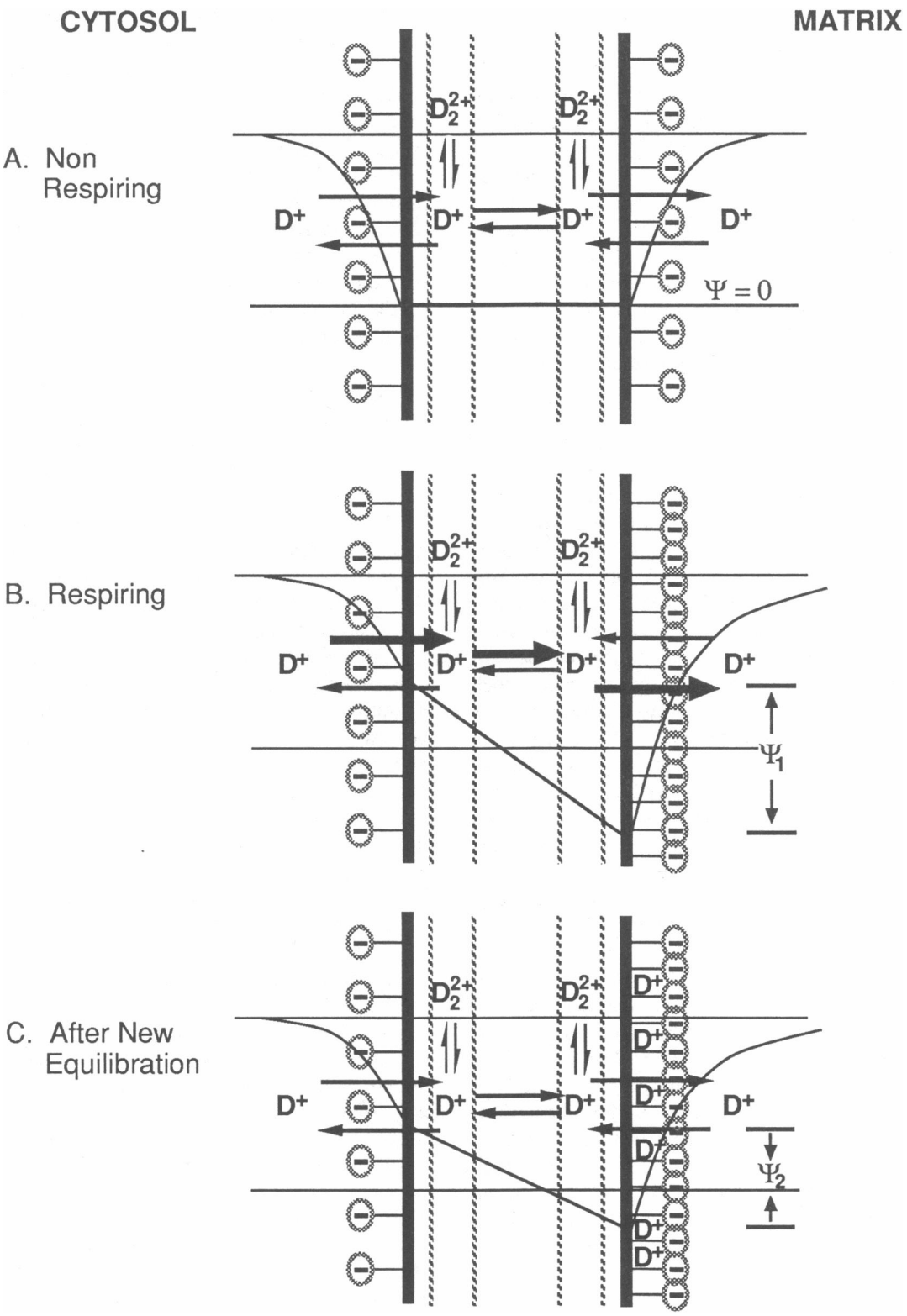

FIGURE 10 Conceptual model of lipophilic cationic dye interaction with mitochondrial membrane. See text for details.

the external face of the bilayer. A single dose estimate of the value of K can be obtained from the potential independent partition of dyes given in Table 1. This gives the number of moles of dye taken up by a 0.1 mg/ml sample. After the initial high concentration of the entering cation in a region just interior to the fixed anionic surface charge, there is a barrier to diffusion to the matrix surface. This barrier is the result of higher viscosity of the lipid and a counter force on the mobile cation from a positive dipole potential in the lipid interior. This positive potential arises from the dipolar nature of the lipid heads and the concentration of cationic charge in the double layer at a Debye length into the aqueous phase from the fixed anionic surface charge (34). With time the dye will equilibrate at the faces depending on their relative solubility on either side and the degree of aggregation forced by the microenvironment.

The degree of fluorescence quenching will depend primarily on the amount of dye sequestered into the aqueous–lipid interface and the extent of dimerization, which is assumed to be the necessary mechanism of quenching. Inner filter effects on fluorescence owing to the high local concentration of fluorophores potentially offers another quenching mechanism, but calculations using an average mitochondrial radius of 0.25 μm as an estimate of the "cell path length," 10 mM for the final inner mitochondrial concentration of dye, extinction coefficients typical of the dyes, and overlap of absorption and fluorescence spectra suggest that <1% of the quenching observed could be accounted for in this manner. The true dimerization constant in the bilayer will most likely differ from the dimerization constants measured for the dyes diluted in aqueous medium of low ionic strength. That dimerization does occur has been directly substantiated by observation of dimerization in changes in both absorption and emission spectra of cationic amphiphilic chromophores interacting with polarized lipid bilayers (11, 35). A thermodynamic consideration of the effect of dye sequestration into an environment which is lipidic and possess a lower dielectric constant predicts that the dimerization should decrease. Correlation between observed titration data and theory give best fits with disaggregation constants slightly smaller than those reported for dyes in low salt aqueous media, however. It appears then that the environment in which the major degree of dimerization is occuring is primarily aqueous with an ionic strength higher than that used for estimate of these constants. This is most likely the aqueous matrix space.

Fig. 10 *B* shows the result of generation of a membrane potential by the respiratory system. A greater surface density of anionic fixed charges is created on the matrix surface than on the cytosolic. This generates a transmembrane potential as the difference between the two surface potentials, negative inside. The dye at the cytosolic aqueous–lipid interface is electrophoresed across the bilayer arriving at the matrix aqueous–lipid interface where it either remains or dissociates into the aqueous matrix space. The decrease in concentration at the cytosolic lipid–aqueous interface is replenished by dye from the incubation mixture. The initial partition constant, K, is thus amplified so that the inner membrane concentration of dye becomes $[\text{Dye}]K(10^{-E/59})$. This is the parameter that is estimated by the Langmuir isotherm analysis which is found to be sensitive both to the partition constant and to the added dye concentration, as expected. At the matrix aqueous–lipid interface the cations equalize the fixed anionic surface charge generated, resulting in a decrease in the transmembrane potential. A limit therefore exists to the amount of dye that can be taken up by a given concentration of mitochondria, a fact observed experimentally by fluorescence titration and modeled by the combination of the equations of Tomov (13) and Heyer et al. (22).

The combined Tomov–Heyer equations predict the quenching ratio (ϵ) as a function of estimable physical constants of the system: the initial transmembrane potential, the initial charge excess on the matrix surface, the dye disaggregation constant, and the partition constant for amphiphilic cation into lipid, β (charges per cm^2/M). β is the most difficult value to estimate because its definition is in terms of the surface concentration of dye necessary to negate a fixed matrix surface anionic charge. Heyer et al. (22) measured values for β between 4.2×10^{15} and 2.4×10^{17} for nonyl to dodecyl *N*-tetramethylamine into a phosphatidylglycerol cholesterol (50%:50%) lipid bilayers. The mitochondrial system is more complex, however, and it would be hard to expect for every mole of dye absorbed into the mitochondrial system one mole of inner matrix surface charge is negated. Some of the dye will localize in regions where it is inaccessible to the inner matrix surface charge. Thus, when β is estimated from the potential independent partition data for DiSC2(5) (Table 1) with the assumption that every dye molecule sequestered into the mitochondria negates an inner matrix surface charge, a value of β of 1.8×10^{19} charges per cm^2/M is calculated, far greater than β measured for the quaternary amino-alkanes. Assuming the larger value for β obtained by Heyer et al. for QA-alkanes, 2.4×10^{17}, an effective fraction of total dye sequestered that reaches matrix membrane surface is then estimated at 0.013. Solutions of the Heyer–Tomov equations suggest that (Fig. 9) a β between 2.4 and 7.0×10^{17} (assuming K_{Dm} of 1×10^{-5} M, $E_o = -200$ mV [36], and [mito] = 0.1 mg/ml), yields an agreement between theoretical and observed fluorescence quenching vs. [Rh123] titration of 0.1 mg/ml respiring mitochondria. This value for β is more in general agreement with those reported or calcu-

lated from reported partition data (27, 28). The data acquired suggest that the ability of a given dye to alter membrane potential is a function of lipid solubility, as theoretically mirrored in the value of β. This is suggested in Fig. 7 by differences in the inhibition of Rh123 binding by other dyes. The dye concentration of competing dyes causing 50% inhibition of Rh123 binding correlates with the degree of energy independent partition seen in absence of membrane potential (Table 1). Rh6G, possessing a greater partition into nonrespiring mitochondria than does Rh123, requires a smaller dose to inhibit Rh123 binding than the relatively nonpartitioning oxazine 1. Also, the Langmuir parameters obtained on respiring mitochondria, compared at equal dye concentration of 1 μM, show Rh6G more avid ($K_d = 1.8 \times 10^{-7}$) than Rh123 ($K_d = 4.8 \times 10^{-7}$) (Table 2). This comparison suggests that the membrane potential is reflected through the potential independent partitionability of the dye. At the same time, the maximum number of sites available is lower (25 vs. 48 nmol/mg). The reduction in apparent binding sites may be due to an earlier negation of transmembrane potential by the more avidly incorporated Rh6G per milligram of mitochondria added.

The comparison between the gravimetric partition of cationic lipophilic dyes and the corresponding change in fluorescence intensity (Table I) elucidates the parameters that are important for the selection of fluorescent cations optimized for reporting membrane potential changes. A high degree of dimerization is essential for maximizing the dynamic range of response upon alteration of membrane potential. There is an upper limit to the aggregation that can be practically used, however, because the dye added external to the mitochondria should itself be primarily in the monomeric state. Thus, dyes with disaggregation constants of the same magnitude as the bulk concentration will be 50% aggregated and so are not expected to react to a potential change with fluorescence quenching. Another requirement of a potential sensitive fluoroprobe is a reasonable (but not too high) partitionability into the mitochondria aqueous–lipid interface in the absence of a membrane potential. Should the dye have no lipid partitionability, the membrane potential would allow only for the concentration of the dye in the cationic double layer at the cytosolic surface of the mitochondrial membrane. That volume is not limiting, however, and it is hard to imagine that the conditions would prevail for dimerization of many molecules. If, on the other hand, the potential independent partition is too high (as with Nile blue A), then either the membrane function may be disrupted entirely, or sufficient anionic surface charge is negated so that the effective membrane potential is substantially decreased. Once a dye is sequestered into the aqueous-lipid surface area, it may bind to other elements there so that dimerization and quenching of the dye is not seen, e.g., DiSC2(3). Although its binding has a high fraction of potential dependent uptake, the interaction yields no measurable quenching. Other dyes, such as oxazine 4 and thionin, neither bind nor quench.

Uptake of dye has direct effects on the function of the respiratory activity (Table 2). Our own observations confirm earlier more complete analysis of the effect of cationic dye addition on the inhibition of oligomycin-sensitive ATPase performed by Mai and Allison (37). They found that some of the dyes exhibit uncoupling activity when added to intact rat liver mitochondria, stimulating both state IV respiration and latent ATPase activity. We find in agreement that all dyes stimulate state IV respiration at a 10 μM/mg dye to mitochondria ratio and that in general they uncouple respiratory stimulation upon addition of ADP. Some dyes (CV, Ox4, NBA) completely uncouple respiration from phosphorylation, but without major alteration of respiratory rate. One mechanism to account for these effects is via the alteration in the transmembrane potential which appears to occur as dye is added. Since F_0F_1ATPase requires a transmembrane potential as the major component of protomotive force for proper operation, reduction of the membrane potential by the cationic dye would be expected to affect the ATPase activity. To support this contention, some correlation is seen between the concentration of dye necessary to half-maximally inhibit F_0F_1ATPase (Table I in Mai and Allison) and the concentration of dye necessary to reduce Rh123 uptake by half (Fig. 7).

Finally, a consideration of alternative explanations for the saturability and toxicity of cationic dye binding to mitochiondria is in order. As stated, a major assumption of the model presented is that the ionic diffusion potential is not altered by the addition of dye. It is not clear exactly how the diffusion potential, if any, is created in the mitochondria. Similarities in the concentration of potassium ion in matrix and cytosol (25, 38) argue against its being the ion whose diffusion sets up the diffusion potential. Possibly calcium ion creates this potential; however, it is known that the matrix concentration of free diffusible calcium ion is kept very low, even lower than the surrounding cytosol, requiring ATP-activated ports for externalization of the ion from the matrix to cytosol (39). Thus it is not clear how its diffusion across the mitochondrial inner membrane could be created by Ca outward flux. It is observed that addition of calcium ions to SSB buffer suspensions of mitochondria causes displacement of cationic dye binding in a fashion indicative of competitive inhibition (40, data not shown). Thus calcium ion concentration differences across the mitochondrial membrane appear to modulate the apparent membrane potential. In the experiments presented, EGTA was present in the medium to maintain a low level [Ca] in the cytosolic

compartment. Under these conditions and in the presence of nontoxic Rh123, the dye binding is seen to be constant for up to 5 h. It is possible that continued addition of dye in some way affects the diffusion of Ca so as to alter the diffusion potential. To rule out this possibility would require measurements of calcium efflux as a function of dye addition. However, it is hard to see how a change in nonlipophilic cationic flux could be modulated so completely by the addition of a lipophilic species except by alteration of the lipid structure so as to short-circuit the calcium-membrane resistance. If this were the case, the dye should very rapidly cause loss of internal calcium in short order followed by total collapse of the membrane potential when all internal calcium has leaked out to the system as is seen when valinomycin is added to mitochondria suspended with dye in SSB having low $[K]$. We do not observe such an effect. Once a particular concentration of dye has bound to the mitochondria, even if it is at a self-inhibitory concentration, the observed quenching, ergo the membrane potential, is stable in SSB/EGTA for many hours. Although these arguments do not rule out the possibility of modulation of diffusion potential, they do raise questions that need to be answered.

The model presented here may be useful toward the organization of observations of dark and phototoxicity of amphiphilic cationic dyes used as photodynamic therapeutic agents. For example, Rh6G is known to exhibit significant cellular dark toxicity as compared to Rh123 at equal incubation doses (41), but the reason for such differences was not clear, as both are apparently well sequestered. The observations above suggest that a greater membrane potential-independent partition for Rh6G than Rh123 results in a greater reduction of membrane potential and a longer effect of the more lipophilic molecule on the membrane function. With the identification herein of measurable parameters of cationic lipophilic species' interaction with mitochondria, a correlation of photodynamic activity of the dyes with these parameters may give a deeper understanding of the mechanisms of photodynamic action.

This work was supported in part by a grant from the Baylor Research Foundation Medical Cell Biology Fund and from the Office of Naval Research (ONR N000014-86-K-0186.

Received for publication 2 March 1989 and in final form 24 July 1989.

REFERENCES

1. Michaelis, L. 1900. Die vitale Farbung, eine Darstellungsmethode der Zellgrana. *Arch. Mikrosk. Anat.* 55:558–577.
2. Conn, H. J. 1977. Biological Stains, 9th edition. Williams & Wilkins Co., Baltimore. 326–363, 409–410.
3. Lewis, M. R., H. A. Sloviter, and P. G. Goland. 1946. In vivo staining and retardation of growth of sarcomata in mice. *Anat. Rec.* 95:89–96.
4. Johnson, L. V., M. L. Walsh, and L. B. Chen. 1980. Localization of mitochondria in living cells with rhodamine 123. *Proc. Natl. Acad. Sci. USA.* 77:990–999.
5. Chen, L. B., I. C. Summerheyes, L. V. Johnson, et al. 1982. Probing mitochondria in living cells with rhodamine 123. *Cold Spring Harbor Symp. Quant. Biol.* 46:141–155.
6. Bernal, S. D., T. J. Lampidis, I. C. Summerheyes, and L. B. Chen. 1982. Rhodamine 123 selectively reduces clonal growth of carcinoma cells in vitro. *Science (Wash. DC).* 218:1117–1119.
7. Lampidis, T. J., S. D. Bernal, I. C. Summerhayes, and L. B. Chen. 1983. Increased rhodamine 123 uptake by carcinoma cells. *Cancer Res.* 43:716–720.
8. Lampidis, T. J., Y. Hasin, M. J. Weiss, and L. B. Chen. 1985. Selective killing of carcinoma cells in vitro by lipophilic-cationic compounds: a cellular basis. *Biomed Pharmacother.* 39:220–226.
9. Castro, D. J., R. E. Saxton, H. R. Fetterman, and P. H. Ward. 1988. Phototherapy with argon lasers and Rhodamine-123 for tumor eradication. *Otolaryngol. Head Neck Surg.* 98:581–588.
10. Oseroff, A. R., D. Ohuoha, G. Ara, et al. 1986. Intramitochondrial dyes allow selective in vitro photolysis of carcinoma cells. *Proc. Natl. Acad. Sci. USA.* 83:9729–9733.
11. Sims, P. J., A. S. Waggoner, C.-H. Wang, and J. F. Hoffman. 1974. Studies on the mechanism by which cyanine dyes measure membrane potential in red blood cells and phosphatidylcholine vesicles. *Biochemistry.* 13:3315–3330.
12. Loew, L. M., L. Benson, P. Lazarovici, and I. Rosenberg. 1985. Fluorometric analysis of transferable membrane pores. *Biochemistry.* 24:2101–2104, 1985.
13. Tomov, T. T. 1986. Pyronin Y as a fluorescent probe for quantitative determination of the membrane potential of mitochondria. *J. Biochem. Biophys. Methods.* 13:29–38.
14. Emaus, R. K., R. Grunwald, and J. J. Lemasters. 1986. Rhodamine 123 as a probe of transmembrane potential in isolated rat-liver mitochondria: spectral and metabolic properties. *Biochim. Biophys. Acta.* 850:436–448.
15. Birge, R. R., editor. 1987. Kodak Laser Dyes. Kodak Publication JJ-169. Eastman Kodak Company, Rochester, NY.
16. Berlman, I. B. 1971. Handbook of Fluorescence Spectra of Aromatic Molecules, 2nd edition. Academic Press, Inc., New York.
17. Rickwood, D., M. T. Wilson, and V. M. Darley-Usmar. 1987. Isolation and characterization of intact mitochondria. *In* Mitochondria: A Practical Approach. V. M. Darley-Usmar, D. Rickwood, and M. T. Wilson, editors. IRL Press, Washington, DC. 1–16.
18. Lowry, Q. H., N. J. Rosenbrough, A. L. Farr, and R. J. Randall. 1951. Protein measurement with the folin phenol reagent. *J. Biol. Chem.* 193:265–275.
19. Pullman, M. E., H. S. Penefsky, A. Datta, and E. Racker. 1960. Partial resolution of the enzymes catalyzing oxidative phosphorylation. I. Purification and properties of soluble, dinitrophenol-stimulated adenosine triphosphatase. *J. Biol. Chem.* 235:3322–3329.
20. Estabrook, R. W. 1963. Mitochondrial respiratory control and the polarographic measurement of ADP:O ratios. *Methods Enzymol.* 6:41–47.

21. Harris, E. J., and K. van Dam. 1968. Changes of total water and sucrose space accompanying induced ion uptake or phosphate swelling of rat liver mitochondria. *Biochem. J.* 106:759–766.

22. Heyer, E. J., R. U. Muller, and A. Finkelstein. 1976. Inactivation of monazomycin-induced voltage-dependent conductance in thin lipid membranes. *J. Gen. Physiol.* 67:703–729.

23. Hashimoto, K., and H. Rottenberg. 1983. Surface potential in rat liver mitochondria: terbium ion as a phosphorescent probe for surface potential. *Biochemistry.* 22:5738–5745.

24. Hashimoto, K., P. Angiolillo, and H. Rottenberg. 1984. Membrane potential and surface potential in mitochondria: binding of a cationic spin probe. *Biochim. Biophys. Acta.* 764:55–62.

25. Rossi, E., and G. F. Azzone. 1969. Ion transport in liver mitochondria: energy barrier and stoicheometry of aerobic K translocation. *Eur. J. Biochem.* 7:418–426.

26. McLaughlin, S. 1977. Electrostatic potentials at membrane-solution interfaces. *Curr. Top. Membr. Transp.* 9:71–144.

27. McLaughlin, S., and H. Harary. 1976. The hydrophobic adsorption of charge molecules on bilayer membranes: a test of the applicability of the Stern equation. *Biochemistry.* 15:1941–1948.

28. Gibrat, R., H. Barbier-Brygoo, J. Guern, and C. Grignon. 1985. Membrane potential difference of isolated plant vacuoles: positive or negative? I. Evidence for membrane binding of cationic probes. *Biochim. Biophys. Acta.* 819:206–214.

29. Bashford, C. L., and J. C. Smith. 1979. The determination of oxonol-membrane binding paramaters by spectroscopic methods. *Biophys. J.* 25:81–85.

30. West, W., and S. Pearce. 1965. The dimeric state of cyanine dyes. *J. Phys. Chem.* 69:1894–1903.

31. Rabinowitch, E., and L. F. Epstein. 1941. Polymerization of dyestuffs in solution: thionine and methylene blue. *J. Am. Chem. Soc.* 63:69–78.

32. Beers, Y. 1962. An Introduction to the Theory of Error, 2nd edition. Addison-Wesley, Inc., Reading, MA. 33–35.

33. Glantz S. A. 1981. Primer of Biostatistics. McGraw-Hill Book Co., Inc., New York. 76–81.

34. Hladky, S. B. 1974. The energy barriers to ion transport by nonactin across thin lipid membranes. *Biochim. Biophys. Acta.* 352:71–85.

35. Grzesiek, S., H. Otto, and N. A. Dencer. 1989. ΔpH induced fluorescence quenching of 9-aminoacridine in lipid vesicles due to excimer formation at the membrane. *Biophys. J.* 55:1101–1109.

36. Mitchell, P. and J. Moyle. 1969. Estimation of membrane potential and pH differences across the cristae membrane of rat liver mitochondria. *Eur. J. Biochem.* 7:471–484.

37. Mai, M. S., and W. S. Allison. 1983. Inhibition of an oligomycin-sensitive ATPase by cationic dyes, some of which are atypical uncouplers of intact mitochondria. *Arch. Biochem. Biophys.* 221:467–476.

38. Campbell, A. K. 1983. Intracellular Calcium, Its Universal Role as Regulator. John Wiley & Sons, New York. 477.

39. Bygrave, F. L., P. H. Reinhart, and W. M. Taylor. 1985. Mitochondrial calcium fluxes and their role in the regulation of intracellular calcium. *In* Calcium and Cell Physiology. D. Marme, editor. Springer-Verlag, Inc., New York. 94–103.

40. Lotscher, H.-R., K. H. Winterhalter, E. Carafoli, and C. Richter. 1980. The energy-state of mitochondria during the transport of Ca^{2+}. *Eur. J. Biochem.* 110:211–216.

41. Wiseman, A., T. K. Fields, and L. B. Chen. 1985. Human cell variants resistant to rhodamine 6G. *Somatic Cell Mol Genet.* 6:541–556.